This paper compares three different surface wave measurement and dispersion methods and applies them to real data. The methods include: (1) a data transformation method based on the wavelength/depth (W/D) relationship that was developed and presented by the first author in another paper; (2) a laterally constrained inversion; (3) a traditional dispersion curve analysis based on interstation measurements. I am only familiar with the third method. The advantages of the first one is that it is a lot faster than the other two and it enables to constrain VP. Overall, the paper needs some reorganization. Too many sections and subsections that are too short. Some will need to be expanded (there is very little motivational background about the region where the methods are applied, description of the models, or geological implications). Considering the new method was already presented in a separate paper, this paper should not be yet another technique paper and needs to be more than that. It is fine to compare with other methods (though perhaps it should have been done in the previous paper), but there needs to be more than that here. It would be good to reframe the paper and focus on the geological problem that is tackled and fold the method comparison into it.

Dear topical Editor,

Thank you for the time you spent reviewing our manuscript and for the useful remarks.

This site was selected to perform a research seismic campaign by Gallego Technic Geophysics and TotalEnergies to mainly test the feasibility and efficiency of the carpet recording and also to calibrate the processing tools for this type of survey layout. In a simplified explanation, carpet recording involves the use of dense receiver spread and limited number of shot locations in easily accessible places (Lys et al., 2018). It is noteworthy to mention that the carpet recording is designed for seismic exploration, and the expressions “dense receiver spread” and “limited number of shots” should be interpreted within this context. The carpet recording workflow was created to facilitate seismic measurements in remote areas such as forests and foothills. An example of carpet recording with irregular receiver grid has been also shown in (Khosro Anjom et al., 2019). The use of sources only in accessible locations makes the acquisition extremely efficient but creates irregular source-receiver layout that demands revalidation of the processing workflow. The primary aim of this study was to fine-tune, adapt, and assess the workflows for characterizing near-surface of a hard rock site when seismic data is collected through a carpet recording scheme. The possibility of retrieving reliable near-surface velocity models is important in the view of seismic processing that aim at correcting the deep exploration data for the effect of weathering layer, such as static corrections (Marsden, 1993; Cox, 1999). For this purpose, we applied three surface wave methods and compared their results with each other and with the available outcrop map. We adapted the multi-channel dispersion curve estimation to irregular source-receiver layout from the carpet recording. These dispersion curves were the inputs to WD and LCI methods. On the other hand, the irregular geometry of the source-receivers’ were advantages toward the surface wave tomography and resulted in homogenous and dense azimuthal coverage, an important property for high-resolution tomographic inversion. In the revised manuscript, we will clarify in detail the motivation behind this research.

The area was chosen as a suitable place to test the carpet recording. To our knowledge, the geological information about the area is limited to the outcrop map in the manuscript that we obtained from French geological survey platform (BRGM). In the revised manuscript, we further analyze the results and draw a more comprehensive comparison to the geological map.

In the beginning, we created the outline of the manuscript so that the three methods can be easily followed by the reader. We now realize that some of the chapters are short, and it would be better to merge certain sections and add more information. These changes will be made to the revised manuscript.

In the following, we provide point-to-point response to all your remarks and comments.

Best Regards,

Authors

Comment R2-1: Section 2 is a little short. It would be useful to give some more background about the location. What previous studies have been conducted? What have they found? What are the remaining issues you can solve with your technique?

Thank you for your useful comment. As we mentioned above, this test site was selected to carry out the acquisition of a research experimental seismic survey mainly to test the feasibility and the efficiency of the carpet recording. To our knowledge besides the outcrop map in the submitted manuscript no other information is available and further geophysical measurements are not in reach. In the revised manuscript, we will clarify the objectives of this survey and what is the main target of the research.

Comment R2-2: Figs. 1 and 2: Please, add latitude and longitude markers on the figures:

Thank you for this comment. According to our agreement for the use of the data, we cannot disclose the exact latitude and altitude of the location, and of the source-receiver positions. Regarding the model estimations, we also had to scale the UTM coordinates to a new reference system for confidentiality.

Comment R2-3: Section 4.2:

- **Comment R2-3a:** Please, specify if the Monte Carlo inversion is linear or non-linear. If it is linearized, please comment on how this can affect the solution.

We use the 1D Monte Carlo algorithm developed by Socco and Boiero (2008). In this method, the VS, Poisson's ratio, and thicknesses are uniformly sampled within the defined model space, and the best fitting models are selected according to a statistical Fisher test. It is noteworthy to mention that the algorithm developed by Socco and Boiero (2008) takes advantage of scaling properties of dispersion curves. The synthetic DCs of the random models are computed and shifted as close as possible to the experimental DC. Then, the scaling factor is obtained from the DC shift and the models are scaled. These scaling steps, which are performed in a fully automatic manner, highly optimize the model space sampling, and reduce the number of required simulations to find the inversion results. The best fitting models are then selected according to a statistical Fisher test with a certain level of confidence. No linearization is introduced in any step of the MC inversion. Since the MC inversion is just a way to carry out one step of the workflow and the MC algorithm is widely described in the original paper, we decided not to go into the details about it.

- **Comment R2-3b:** Density is considered a priori. How? Please describe what kind of constraint is imposed. A fixed value? A fixed ratio? Something else? Justify the choice.
  It has been shown in many previous studies that even though density is a model parameter according to Haskell and Thompson's forward modelling of the surface wave dispersion curve, it has a minor impact on the simulated phase velocity (Xia et al., 1999; Foti and Strobbia, 2002; Pan et al., 2018). We assume the density according to the available information of the site. The Aurignac site is characterized by hard rock. We assumed density of 2000 kg/m^3 for the first layer and 2200 kg/m^3 for the other layers.

- **Comment R2-3c:** Line 145: "wide model space" is a vague statement. Please quantify by giving the bounds of your model space. Have you tried to modify the bounds of the model space and see how it affects the solution?

Thank you for this insightful comment. In the revised manuscript, we will provide the upper and lower boundaries of the VS model. The Poisson's ratio of the layers was sampled between 0.1 to 0.45 for all layers, and the density was fixed as mentioned in Comment R2-3b.

Yes, we have tested various boundaries not only for this data set but for other data sets in Khosro Anjom et al. (2019), Khosro Anjom (2021). The algorithm is very efficient given that it scales the sampled models according to the misfit between experimental and synthetic dispersion curves (Socco and Boiero, 2008). Hence, if the model space boundaries are inappropriate the sampling automatically gets out of them. Figure R3 below shows an example of how the models are automatically moved beyond the initial boundaries when the boundaries were selected poorly with respect to the data. Moreover, thanks to the parallel computing of the code, we sampled a large number of models within reasonable time (1,000,000 in this manuscript), which further increases the independence of the final results with respect to defined model space.

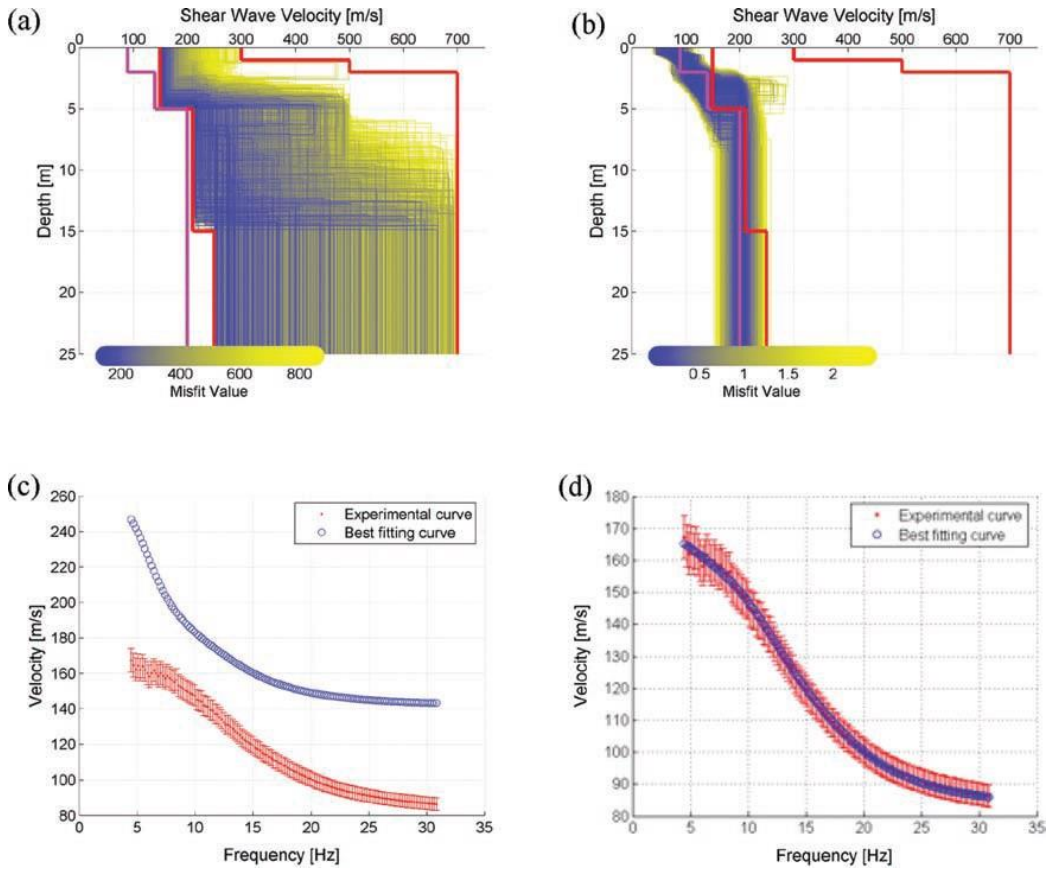

Figure R3: *A synthetic example showing the impact of model scaling in the final results of the MCI (from Socco and Boiero, 2008). (a) and (b) 5,000 best fitting models from 200,000 sampled models for a three-layer model (magenta): (a) without scaling; (b) application of the scale properties; the homogeneous boundaries (red lines) have been on purpose selected not to contain the true model; (c) and (d) best fitting dispersion curve compared with the experimental one: (c) no scaling; (d) application of the scale properties.*

- **Comment R2-3d**: What criteria did you apply to select the models with the Fisher test?

Each synthetic dispersion curve has a misfit with respect to the experimental DC computed as (Socco and Boiero, 2008):

$$S = \frac{\sum_{i=1}^{l}\left[\left(v_{s,i}-v_{e,i}\right)^2 \sigma_{e,i}^2\right]}{l-(3n-1)}, \qquad \text{(R1)}$$

where $v_{s,i}$ and $v_{e,i}$ are the elements of synthetic and experimental phase velocities, $\sigma_{e,i}$ are the elements of data uncertainty vector obtained in DC picking stage, l is the number of data points, and n is the number of layers in the inversion. Since the VS, Poisson's ratio and thickness are the variable of the inversion the model parameters are equal to $3n-1$. The Fisher test is applied to these misfits to select the best fitting models, considering a level of confidence. We used a low level of confidence equal to 0.001 to include in the results all geological settings that are providing a good fitting with the

experimental dispersion curves. In Figure R4 below, an example of three different levels of confidence for the inversion of an experimental dispersion curve is shown (from Socco and Boiero 2008).

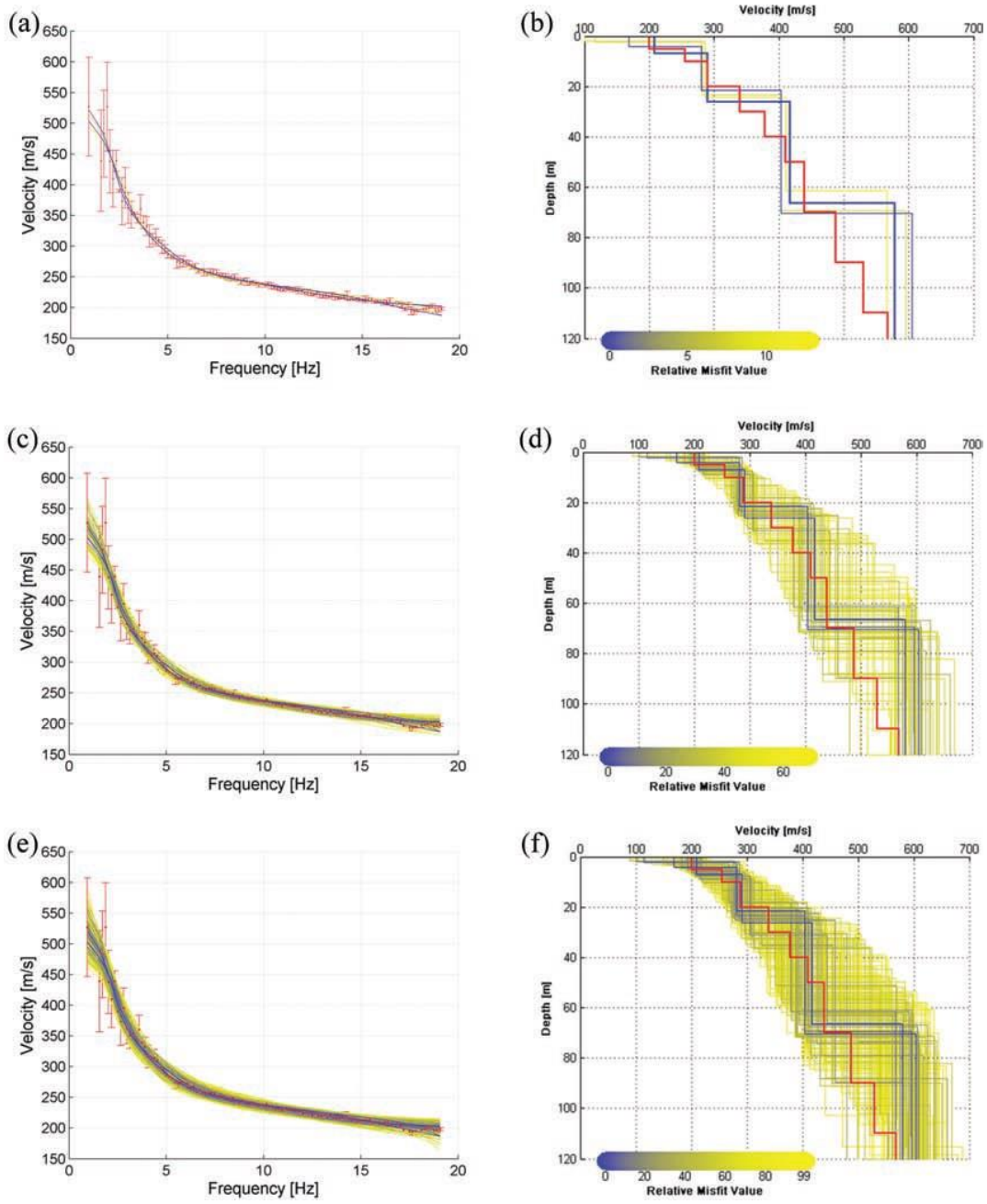

Figure R4: *The selected models from the Monte Carlo inversion of an experimental dispersion curve using different levels of confidence equal to a) 0.25, b) 0.01, and c) 0.001. The figure is taken from Socco and Boiero (2008).*

- **Comment R2-3e:** "The experimental W/D relationship is significantly sensitive to Poisson's ratio." Please, demonstrate or provide a reference to justify this statement.

Thank you for this comment. Numerous tests have been performed to show the sensitivity of the W/D relationship to Poisson's ratio (Comprehensive analysis has been previously published in Socco and Comina, 2017; Khosro Anjom, 2021; Khosro Anjom et al., 2019). In Figure R5 below, as an illustration we show the synthetic simulation Khosro Anjom (2021) performed to evaluate the sensitivity of the wavelength-depth relationship to Poisson's ratio. The VS (Figure R5a) and density of the model were kept constant, and only the Poisson's ratio was changed to evaluate Poisson's ratio's impact on the wavelength-depth relationships. Figure R4b shows significant variation of the estimated wavelength-depth relationships. In this plot the color shows the Poisson's ratio corresponding to each wavelength-depth relationship

In Figure 6d and 7d of the submitted manuscript also sketches the sensitivity of the reference data for cluster 1 and 2 with respect to Poisson's ratio. In the revised manuscript, we will provide more references to this aspect.

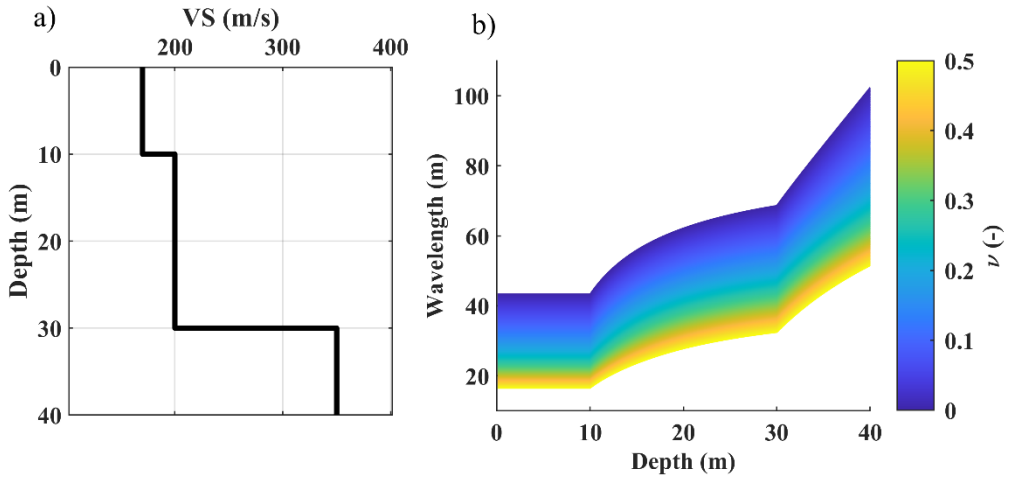

Figure R5: *A synthetic study to evaluate the sensitivity of wavelength-depth relationship with respect to variations in Poisson's ratio (from Khosro Anjom, 2021). a) The S-wave velocity of the synthetic model. b) the computed wavelength-depth relationships from different Poisson's ratio.*

- **Comment R2-3f:** It would be very useful to see a plot of sensitivity curves at the measured periods

Thank you for the comment. Within the scope of the W/D data transform no inversion is carried out and the dispersion data are directly transformed to shear wave velocity models. Let us know if we misunderstood your remark or you intended this comment about the sensitivity matrices of LCI or SWT.

- **Comment R2-3g:** In Figs. 6 and 7, VSZ was not defined

Thank you for this comment. The VSZ is the time-average VS. In the revised manuscript we replace it with time-average VS that is used in the manuscript. We also better clarify that time-average VS profiles are computed from the layered velocities.

- **Comment R2-3h:** Fig. 8 is based on one model only. It would be useful to plot and discuss the uncertainties in each Vs and Vp model and how they propagate into Poisson's ratio uncertainties. Without good error estimates, differences between clusters are not meaningful.

Thank you for this comment. Figure R6a below shows the computed Poisson's ratio cube from estimated VS and VP models of the W/D method. Separately for each cluster, we used these estimated Poisson's to obtain a standard deviation at each depth. In Figure R6b and R6c, we added these standard deviations to the estimated Poisson's ratio for each cluster as you suggested. In the revised manuscript, we will add these errorbars to the estimated Poisson's ratios of the Figure 8c and 8d of the submitted manuscript. The estimated Poisson's ratios for the two clusters are used as prior information in the LCI and SWT methods, and for the conversion of the estimated VS models from these methods to VP.

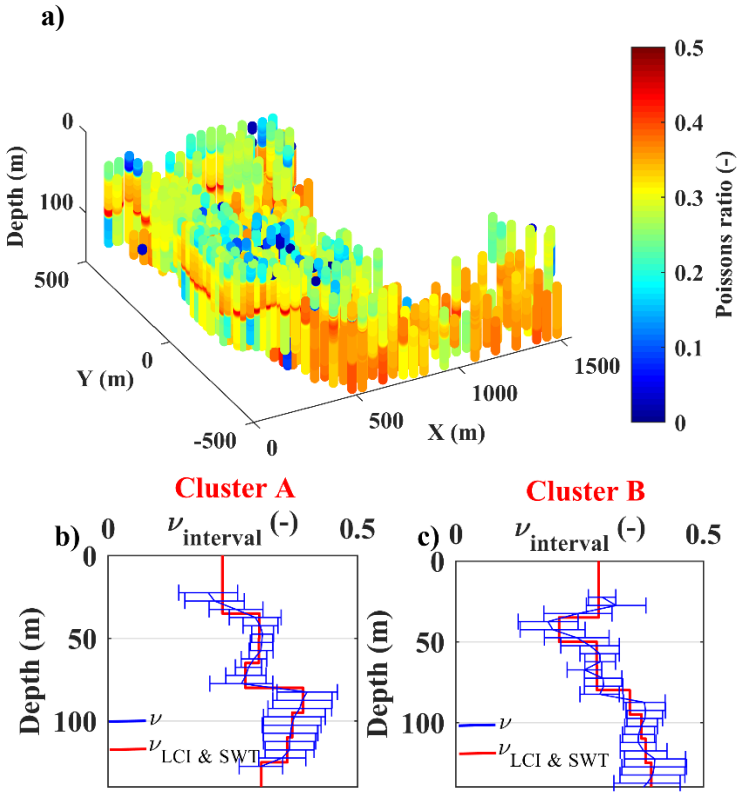

Figure R6: *Uncertainty estimation for the reference Poisson's ratios from W/D method. a) 3D view of the obtained Poisson's ratio from W/D method. b and c) Estimated Poisson's ratio from the reference estimated VS and VP model of the W/D method for cluster 1 and 2; The standard deviations were obtained from all estimated Poisson's ratio of each cluster in Figure R5a.*

Comment R2-4: Section 4.3 is very short and may need to be expanded or folded into another section.

We had intentionally separated the three-methods application and had kept them short to facilitate the comparison by the reader. In the revised manuscript, we merge the methods together in a single chapter. Thank you for the comment.

Comment R2-5: Section 5.2

- **Comment R2-5a:** VP and density are fixed a priori: how? Details are needed

As we mentioned in response to comment R2-3b, the density has minor impact on the inversion results. It is a standard approach in surface wave analysis for near-surface characterization to use fixed density based on information of the site. As we mentioned in response to comment R2-3b, we considered density of 2000 kg/m^3 for the first layer and 2200 kg/m^3 for the rest of the layers.

On the other hand, the VP is not fixed. As we mentioned in response to comment R2-3h, we estimated two reference Poisson's ratio for the two clusters (zones) using the W/D method (Figure R5b and R5c above). We used one of the two estimations of Poisson's ratio for each model point in scheme of LCI and tomographic inversion, based on its location. We will clarify these aspects in the revised manuscript.

- **Comment R2-5b:** Line 221: What does "contemporarily" mean in this context? I suspect it is incorrect English usage.

Maybe the word simultaneously was a more proper word as we meant that we invert the dispersion curves all together, opposed to one-by-one 1D inversions. In each iteration a single sensitivity matrix is computed and used to update all model parameters. In the revised manuscript, we will rephrase the sentence to eliminate the confusion.

- **Comment R2-5c:** What are the lateral constraints applied?

We used the same level of lateral constraints equal to 50 m/s in both LCI and SWT methods. Both algorithms are designed to allow lateral and vertical constraints, as well as constraints by a priori information. We only used lateral constraints in these inversions. Both inversions are in scheme of damped least-square deterministic scheme to minimize the misfit. The misfit Q is defined as:

$$Q = \left[(\mathbf{d_{obs}} - \mathbf{d(m)})^{\mathbf{T}}\, \mathbf{C_{obs}^{-1}}\, (\mathbf{d_{obs}} - \mathbf{d(m)}\right] + \left[\left(-\mathbf{R_p m}\right)^{\mathbf{T}} \mathbf{C_{Rp}^{-1}} (-\mathbf{R_p m})\right], \qquad \text{(R2)}$$

where the first term determines the misfit between the experimental data $\mathbf{d_{obs}}$ and synthetic data $\mathbf{d(m)}$. $\mathbf{m}$ is the vector of the model parameters and $\mathbf{C_{obs}^{-1}}$ is the reciprocal of the covariance matrix. The second term defines the lateral regularization of the velocities, where $\mathbf{R_p}$ is the regularization matrix composed of values 1 and -1 for the constrained parameters and zeros elsewhere. The strength of the regularization is determined by the covariance matrix $\mathbf{C_{Rp}}$.

Comment R2-6: Section 5.3: Please expand and describe your models

Thank you for this comment. The estimated VS model from LCI, similar to W/D estimated VS model shows a significant change in the trend of the velocity from east to west in the first 87.5 m shown in Figure 11, which is in-line with the geological information from the site (the outcrop map in Figure 19. The high velocity in the east is due to the marl and limestones formations of the Sparnecian and lower Thanetian, whereas the shallow part of the western area is covered by loose material. In the deeper portion of the model below 87.5 m the contrast almost disappears and higher velocity up to 1500 m/s is reached,

probably by reaching Danian formation that is known to have higher velocity than Sparnecian and lower Thanetian. In the submitted manuscript, we will merge the three methods sections to facilitate the description of the models, while avoiding repetitions.

Comment R2-7: Section 6.3: The results need to be described. A paper section should have more than one sentence.

Thank you for this comment. Similar to the estimated models from LCI and W/D methods (comment R2-6), the model from the SWT method depicted significant lateral variation between the east and west within the shallow layers. Nevertheless, the SWT model provides a smoother transition zone between east and west, which is mainly caused by the lateral constraints of the inversion. The level of constraint is a compromise between the sharpness of lateral variations and unrealistic perturbations and inconsistency in the estimated model. A weaker laterally constrained inversion will definitely enhance the sharpness of the transition zone but create unrealistic perturbations to the model (Boiero and Socco, 2010). It is noteworthy to mention that even though the constraints of the LCI and the SWT applications are similar, the SWT provides a smoother model, mainly due to the differences in the covariance matrix of the dispersion data and to the difference in the forward modelling of the synthetic dispersion curves.

Like the other two methods, the estimated VS model from SWT shows no contrast between west and east below 95 m where it reaches the Danian formation. In the revised manuscript, we will provide more description of the estimated models.

Comment R2-8: Section 7:

- **Comment R2-8a:** Again, model comparison would be better with error bars on the individual models.

Thank you for this comment. For two reasons we believe the boxplots are a more reasonable choice to sketch the misfit compared to errorbars between the models from the three methods. First, they provide detailed comparison within different depth and between each two methods. Also, in each location and each depth, we have only three results that are from the three methods. As a result, obtaining an errorbar (standard deviation) for each model point at each depth may be statistically invalid. We prefer to maintain the differences between the models within the scope of the boxplots. If the topical editor believes otherwise provided these explanations, we will prepare the revisions accordingly.

- **Comment R2-8b:** Fig. 18: the caption should explain the difference between blue and red symbols.

In the submitted manuscript, we had provided the explanation of the standard boxplot in the text of the discussion above the figures. We understand that figure caption is a better location to explain the boxplots. Basically, the box plot is defined by three lines showing the 25th percentile, median and 75th percentile of the residual's distribution, and whisker lines extending from the box's edges up to 1.5

times the distance between the edges of the box. The rest of the data are considered as outliers and are shown with "+". We moved this explanation accordingly in the revised manuscript.

- **Comment R2-8c:** A discussion of the geological implications of the results is needed. The short paragraph at the end of the section needs to be expanded.

Thank you for this comment. All three methods depict a contrast between the limestone rich area in the west and loose material in the east. These observations are corroborated by the geological information as was mentioned in comment R2-6 and R2-7. Given the site is an open-cast limestone mining site, the estimated models can offer valuable insights for strategizing the expansion and excavation of the quarry in the investigated zone to support the nearby cement production facility. In the revised manuscript, we will discuss these implications.

Comment R2-9: Section 8: I think saying a method is "a great breakthrough" may be an overstatement. It would be better to use the word "advantageous" or something like that instead.

Thank you for your comment. By *"As a result, the automation of the DC picking can be considered a **great breakthrough in industrialization** of these methods, which enables their fast applications to even larger data sets than the one used in this paper.",* we meant a robust automatic picking algorithm in the future can give a significant boost to the industrialization of the surface wave algorithms. To eliminate any confusion, we will rephrase the sentence as:

"As a result, the automation of DC picking can be viewed as an important milestone in the industrialization of the surface wave methods, facilitating their swift application to data sets even larger than the one used in this study."

Comment R2-10: Minor comments

- **Comment R2-10a:** Overall, a lot of indices, exponents, and subscripts need to be fixed (e.g. VS, VP, density units, etc).
  Thank you for this comment. We will fix these in the revised manuscript.
- **Comment R2-10b:** There are too many subsections that are very short and probably should be combined into bigger sections or be expanded significantly.
  We will reorganize the sections and will remove many of the subsections in the revised manuscript.
- **Comment R2-10c:** Line 38: reference to Socco et al. (2017) needs reformatting
  Thank you. We will fix this issue in the revised manuscript.
- **Comment R2-10d:** I am not familiar with the type of study this is applied to. Why do you calculate a time-average velocity? This needs a bit of context. Do you mean Vs measured at different times? Why would Vs depend on time?
  Thank you for this comment. The time-average velocity at a given depth is the average velocity of the wave (either S- or P-wave) from the surface down to that depth. The time average velocity can be used directly to obtain the traveltime of a wave from the surface down to the specific depth. The term time-average comes from the fact that to obtain an average velocity at a depth, the

traveltime within each layer should be used as the weight to the arithmetic averaging. An illustration of why it is called time-average velocity can be shown as:

$$VSZ\ (z) = \frac{\sum_n h_i}{\sum_n \frac{h_i}{VS_i}} = \frac{\sum_n VS_i.t_i}{\sum_n t_i}, \qquad \text{(R3)}$$

where, h_i, VS_i, and t_i are the thickness VS and traveltime at the ith layer. We hope this explanation clarifies the time-average velocity concept. In the revised manuscript, we will explain more clearly the concept of time-average velocity.

The time average velocity is directly used for many purposes. For instance, in the context of seismic reflection the time average velocity is used for static corrections. These corrections are routinely applied to remove the effect of the weathering layer from the data, whose heterogeneities may represent a significant source of noise (Marsden, 1993; Cox, 1999). In the context of seismic hazard estimation, the time average velocity, also called harmonic velocity by some authors, is a proxy for local seismic response. For instance, VS_{30}, the time average velocity at 30 m depth, is a standard parameter, used in many national and international regulations, to classify sites according to seismic response classes, thanks to the correlation between VS_{30} and PGA (peak goring acceleration). In the W/D method, to retrieve the W/D relationship, the layered model is transformed into its corresponding time-average model (equation R3) and compared with the DC plotted as a function of wavelength.

- **Comment R2-10e:** Line 39: Rephrase “showed with synthetic and real tests” to “showed with synthetic tests and tests on real data”
  Thank you for this comment. We will implement the change in the revised manuscript.

- **Comment R2-10f:** Line 50: mantel should be mantle
  Thank you for this comment. We will implement the change in the revised manuscript.

- **Comment R2-10g:** Line 53: application of SWT for the near-surface characterization➔ application of SWT for near-surface characterization
  Thank you for this comment. We will implement the change in the revised manuscript.

- **Comment R2-10h:** Line 54: In literature ➔ In the literature
  Thank you for this comment. We will implement the change in the revised manuscript.

- **Comment R2-10i:** Line 60:
  - VS should have been defined much earlier in the text
  - “the” S-wave velocity model
  - Remove “the recordings of”. It is the receivers that are aligned with the event. Also, please specify that the alignment is approximately along the great-circle path and thus implies ray theory I applied.

  Thank you for this comment. We will implement the change in the revised manuscript.

- **Comment R2-10j:** Line 66: “on two-station ones.” à “on two-station methods.”
  Thank you for this comment. We will implement the change in the revised manuscript.

- **Comment R2-10k:** Line 71: Incorrect English wording for “that is in advantage of SWT.”
  Thank you for this comment. We will implement the change in the revised manuscript.
- **Comment R2-10l:** Line 8: “the” south of France
  Thank you for this comment. We will implement the change in the revised manuscript.

- **Comment R2-10m:** Fig. 7b: vertical axis label needs to be moved
  Thank you for this comment. We will implement the change in the revised manuscript.

- **Comment R2-10n:** Line 288: analyse ➔ analyze
  Thank you for this comment. We will implement the change in the revised manuscript.

REFERENCES

Boiero, D., and Socco, L.V.: Retrieving lateral variations from surface wave dispersion curves, Geophysical Prospecting, 58, 977-996, https://doi.org/10.1111/j.1365-2478.2010.00877.x, 2010.

Cox, M.: Static Corrections for Seismic Reflection Surveys, SEG, 546, 1999.

Foti, S., and Strobbia, C.: Some notes on model parameters for surface wave data inversion: Symposium on the Application of Geophysics to Engineering and Environmental Problems (SAGEEP), https://doi.org/10.4133/1.2927179, 2002.

Khosro Anjom, F.: S-wave and P-wave velocity model estimation from surface waves, PhD Thesis, Politecnico di Torino, Torino, Italy, https://iris.polito.it/handle/11583/2912984, 2021.

Khosro Anjom, F., Teodor, D., Comina, C., Brossier, R., Virieux, J., and Socco, L. V.: Full-waveform matching of VP and VS models from surface waves, Geophys. J. Int., 218, 1873–1891, https://doi.org/10.1093/gji/ggz279, 2019.

Lys, P.O., Elder, K., Archer, J., and the METIS Team: METIS, a disruptive R&D project to revolutionize land seismic acquisition, in: RDPETRO 2018: Research and Development Petroleum Conference and Exhibition, Abu Dhabi, UAE, 9-10 May 2018, 2018.

Marsden, D.: Static corrections--a review, Part 1: The Leading Edge, 12, 43-49, doi: 10.1190/1.1436912, 1993

Pan, L., Chen, X., Wang, J., Yang, Z., Zhang, D.: Sensitivity analysis of dispersion curves of Rayleigh waves with fundamental and higher modes, Geophysical Journal International, 216, 1276–1303, https://doi.org/10.1093/gji/ggy479, 2019.

Socco, L. V. and Comina, C.: Time-average velocity estimation through surface-wave analysis: Part 2 — P-wave velocity, Geophysics, 82, U61–U73, https://doi.org/10.1190/geo2016-0368.1, 2017.

Socco, L.V., and Boiero, D.: Improved Monte Carlo inversion of surface wave data: Geophysical Journal International, 56, 357-371, doi: 10.1111/j.1365-2478.2007.00678.x, 2008.

Xia, J., Miller, R.D., and Park, C.B., Estimation of near-surface shear-wave velocity by inversion of Rayleigh waves, Geophysics, 64, 691-700, https://doi.org/10.1190/1.1444578, 1999.